Neutron helicity amplitudes

A. V. Anisovich,[1,2] V. Burkert,[3] N. Compton,[4] K. Hicks,[4] F. J. Klein,[5] E. Klempt,[1,3,*] V. A. Nikonov,[1,2] A. M. Sandorfi,[3] A. V. Sarantsev,[1,2] and U. Thoma[1]

[1]*Helmholtz-Institute für Strahlen- und Kernphysik der Rheinischen Friedrich-Wilhelms Universität, Nussallee 14-16, 53115 Bonn, Germany*
[2]*Particle and Nuclear Physics Institute, Orlova Rosha 1, 188300 Gatchina, Russia*
[3]*Thomas Jefferson National Accelerator Facility, 12000 Jefferson Avenue, Newport News, Virginia 23606, USA*
[4]*Department of Physics & Astronomy, Ohio University, Clippinger Lab 251B, Athens, Ohio 45701, USA*
[5]*Department of Physics, Catholic University of America, 200 Hannon Hall, Washington, DC 20064, USA*

(Received 4 August 2017; revised manuscript received 11 October 2017; published 3 November 2017)

The helicity amplitudes for the photoproduction of nucleon resonances excited from neutrons are determined in the Bonn-Gatchina coupled-channel partial wave analysis. Upper limits for the decay fraction of the pentaquark candidate $N(1685) \to K^0\Lambda$ are given. The electric and magnetic couplings at the pole positions are also tabulated, and these are used to suggest candidates for possible multiplets with quark-spin-1/2 and -3/2 content.

DOI: 10.1103/PhysRevC.96.055202

I. INTRODUCTION

The search for *missing resonances* is the driving force for a number of experiments in which the interaction of a photon beam in the GeV energy range with a hydrogen or deuterium target is studied. In quark models [1–3] and lattice calculations [4] numerous resonances are predicted to exist which have failed to show up experimentally. The investigation of photoreactions excited from neutrons is a part of the search for these missing resonances. In both reactions, induced by γp and γn, the same N^* and Δ^* resonances are produced, even though the production strengths of N^* resonances are different; there could even exist resonances that are excited strongly from neutrons but not from protons [5]. But the pole positions of resonances in the complex energy plane, as well as their decay couplings, should be identical, independent of their production. Only the background terms may be (and are) very different. At present, the data base for γp reactions is much richer than the one for γn; data on γn serve to test consistency and to determine the helicity amplitudes for the production of N^* resonances excited from neutrons. The helicity amplitudes of Δ^* resonances are, of course, the same for photoproduction from proton and neutron targets.

The helicity amplitudes for the photoproduction of N^* resonances excited from neutrons have been determined by several groups [6–12]. Mostly, the real-valued helicity amplitudes have been reported from fits using Breit-Wigner representations of resonances. Only the two latest publications [11,12] reported the complex helicity amplitudes at the resonance poles as suggested in Ref. [13]. After these determinations, new high-quality data have been published [14–21] and some data [22] have not been included in the last published BnGa partial wave analysis (PWA) [11]. It now seems appropriate to include the new data in our PWA and to discuss possible changes in the helicity amplitudes.

The paper is organized as follows: we present in Sec. II a table of the data sets used in this analysis: the observables, the number of data points, the reduced χ^2 that had been obtained in the previous fit of Ref. [11], and the χ^2 obtained in the present analysis. In Sec. III we give a short outline of the BnGa PWA method, present the results on helicity amplitudes, and discuss changes in the results. Subsequently, in Sec. IV, we give a short account of a search for a resonance in the 1685-MeV mass range that is advocated in a number of publications [15–19,23–25]. The results on the helicity amplitudes are discussed in Sec. V. The paper ends with a short summary in Sec. VI.

II. THE DATA BASE

Photoproduction off neutrons suffers from the lack of free neutron targets. Instead, deuteron targets are used. This may lead to two unwanted effects: The Fermi momentum distribution may smear out the initial γn invariant mass, and the so-called *spectator* proton may undergo final-state interaction with hadrons emerging from the γn interaction.

The effect of the Fermi motion can be avoided by a full reconstruction of the final state where the momentum of the bound neutron can be determined. Final-state interactions are particularly strong for the np interactions in the $\pi^0 n p_{\text{spectator}}$ final state. For $\pi^- p p_{\text{spectator}}$, the two-proton final state has isospin $I = 1$ while the deuteron has $I = 0$; hence final-state interactions are suppressed [26]. However, polarization observables are affected by interfering spin-dependent amplitudes and can be particularly sensitive to final-state interactions [27]. However, these can be suppressed to a low level by kinematic restrictions, as done in Ref. [21] where a requirement of < 100 MeV/c has been placed on the spectator momentum. There are, of course, no final-state interactions in the reaction $\pi^- p \to \gamma n$, which therefore serves as an important test that the effects of final-state interactions in the $\gamma d \to \pi^- p p_{\text{spectator}}$ reaction are well under control. Final-state interactions appear to have at most very small effects on the cross sections for the reaction $\gamma p \to K^0 \Lambda p_{\text{spectator}}$: the reconstructed momentum distribution of the spectator proton is fully consistent with the distribution expected from the Fermi motion of the proton bound in the initial proton [20]. In this case, a spectator momentum cut at 300 eV/c was applied. The use of different reactions in a coupled-channel fit thus provides hints for hidden effects of final-state interactions; these effects are expected in different kinematic regions when different

*klempt@hiskp.uni-bonn.de

TABLE I. Data on photoproduction from neutrons bound in deuterons are used in this analysis. In the selection of events from photoproduction from nearly free neutrons, either the full kinematics (and thus the momentum of the bound neutron) is measured or a cut on the proton momentum ensures that it acted as a spectator. The symbol (p) stands for $p_{\text{spectator}}$. Listed are the observable, the number of events, and the χ^2/N_{data} in two fits. Two separate entries are given for the $\gamma n \to \pi^- p$ differential cross section as measured in bubble chamber [28,29] and counter [30–36] experiments. The χ^2_{old} shows the quality of the description of γn data in 2013 [11], the χ^2_{new} represents the new description. The η photoproduction results from Ref. [24] have not been included in the new PWA; the new χ^2 shows their inherent incompatibility.

$\gamma d \to \pi^- p(p)$	Observ.	N_{data}	$\chi^2_{\text{old}}/N_{\text{data}}$	$\chi^2_{\text{new}}/N_{\text{data}}$
[28,29]	$d\sigma/d\Omega$	529	3.08	3.06
[30–36]	$d\sigma/d\Omega$	1298	2.32	2.91
[37–45]	Σ	315	3.08	2.98
[46–49]	T	105	3.18	1.97
[50–52]	P	20	3.17	1.50
[21]	E	263	—	1.50
$\pi^- p \to \gamma n$				
[53–59]	$d\sigma/d\Omega$	495	1.53	1.68
[60–62]	P	55	3.11	1.66
$\gamma d \to \pi^0 n(p)$				
[63–66]	$d\sigma/d\Omega$	147	2.98	3.22
[67]	Σ	216	2.89	3.53
[14]	$d\sigma/d\Omega$	969	—	3.38
$\gamma d \to \eta n(p)$				
[24]	$d\sigma/d\Omega$	330	1.40	9.20
[68]	Σ	99	2.17	1.67
[15,16]	$d\sigma/d\Omega$	880	—	1.07
$\gamma d \to K^0\Lambda(p)$				
[20]	$d\sigma/d\Omega$	364	—	1.09
$\gamma d \to K^+\Sigma^-(p)$				
[22]	$d\sigma/d\Omega$	229	—	0.71

reactions are fitted. Thus we are convinced that final-state interaction cannot have a significant effect on our results.

Table I lists the data on photoproduction from quasi-free neutrons that have been used in this analysis, the number of data points, and the χ^2/N_{data} of the best fit. The $\gamma n \to \eta n$ results from Ref. [24] are no longer used in this analysis and are replaced by those presented in Refs. [15,16]. The new data differ substantially from the older ones. In the new data [15,16], the final state is fully reconstructed; hence there is no uncertainty due to Fermi smearing, and the statistics is considerably improved. Within the PWA fits, the new data are more compatible with other data sets, in particular with those on T and P (see Table I). Thus we are convinced that the new data are a better representation of physical reality. When the old data are included in the fit with a very low weight, the $\chi^2/N_{\text{data}} = 6.59$ for the old data shows the incompatibility of the two data sets.

III. PARTIAL WAVE ANALYSIS

The transition amplitude that is used in the present analysis is defined by a multichannel amplitude in the form of a modified K matrix [69]. The modified K matrix takes into account the imaginary and real parts of the corresponding loop diagrams and combines the contributions from resonances and from background processes. Amplitudes representing t-channel exchanges are described as Reggeon exchanges. Explicit formulas are given in Ref. [69]. The full data base includes the real and imaginary parts of the πN multipoles as derived by the George Washington University group [70], and all major results on pion and photoinduced reactions. In the fits described here, masses, widths, decay modes of all resonances, and helicity amplitudes for the production of Δ^* resonances are fixed to values determined by fits to pion-induced and photoproduction reactions with proton targets [71,72]; photoproduction data from neutrons (bound in deuterons with a spectator proton) are used to derive the helicity amplitudes for exciting N^* resonances from neutrons. The data in Table I are used without a normalization factor (in contrast to the data using a proton target). We also made fits that included pion-induced and photoproduction reactions with proton targets and in which the properties of all resonances were varied freely. These fits gave fully consistent results: all values stayed well within the our quoted errors.

Figure 1 shows the differential cross sections for $\gamma d \to K^0\Lambda(p)$ [20] and $\gamma d \to K^+\Sigma^-(p)$ [22]. Figure 2 shows the E asymmetry for $\vec{\gamma}\vec{n} \to \pi^- p$ [21]. The results of the fits—shown by solid and dashed curves in the figures—depend on the starting values for the helicity amplitudes. Two classes of minima are found that have very similar χ^2 but that yield slightly different helicity amplitudes. The fits are close to each other in regions where data exist and differ very significantly in the backward region. Obviously, data at sufficiently large backward angles would easily discriminate between the two solutions.

The total cross sections in Fig. 3 have been obtained by integration of the experimental data over the solid angle, using the PWA prediction where no data exist. In the case of $\gamma n \to K^0\Lambda$, the cross section rises steeply from threshold, reaches about 1.7 μb, and then drops slowly. In contrast to $\gamma p \to K^+\Lambda$, there is no t-channel contribution with kaon exchange (the photon couples strongly to K^+K^- via vector meson dominance but is decoupled from $K^0\bar{K}^0$). In both solutions, the threshold region is dominated by $N(1650)1/2^-$, and large contributions stem from $N(1710)1/2^+$ and $N(1880)1/2^+$. The first solution gives a larger contribution from $N(1900)3/2^+$ and $N(1975)3/2^+$, while the second solution assigns slightly less intensity to these two resonances and more intensity to $N(1710)1/2^+$ and $N(1880)1/2^+$. Both solutions are used in the error evaluation. The data on $\gamma n \to K^+\Sigma^-$ have a better solid angle coverage, and the differences between the two solutions in Fig. 1 are mostly smaller. There is no sign of $N(1650)1/2^-$ in $\gamma p \to K^+\Lambda$ or $K^+\Sigma^-$, but $N(1895)1/2^-$ is seen strongly.

The one-star $N(2100)1/2^+$ resonance is definitely required in the fit; so far it has not yet been reported in $K\Lambda$ decays. The $N(1975)3/2^+$ resonance, first suggested in Ref. [73], improves the fit but its properties are ill-defined. In some solutions, it is found with a mass above $N(1900)3/2^+$, and in some solutions in the 1800- to 1900-MeV region. Here, we include the $N(1975)3/2^+$ helicity couplings but warn the reader that the evidence for this resonance is poor. The

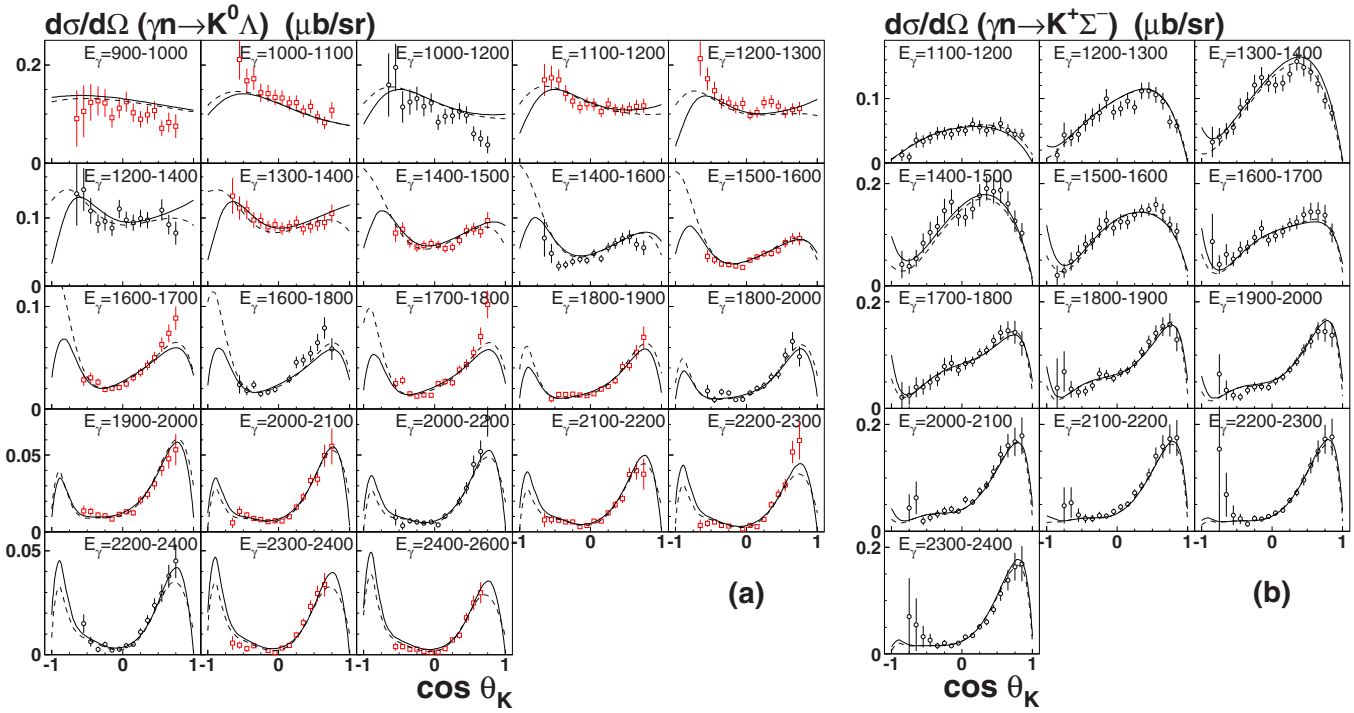

FIG. 1. Left: Differential cross sections for $\gamma d \to K^0\Lambda(p)$. Red squares and black circles represent data from the CLAS g10 and CLAS g13 runs, respectively [20]. Right: $\gamma d \to K^+\Sigma^-(p)$ [22]. The solid and dashed curves show two BnGa fits.

$N(1875)3/2^-$ resonance was reported with large branching ratios for decays into $N\pi\pi$ [74]; here, it contributes very little. The negative-parity resonances $N(2120)3/2^-$, $N(2060)5/2^-$, and $N(2190)7/2^-$ are needed to obtain acceptable fits. The evidence for the high-spin resonances with positive parity, $N(2000)5/2^+$ and $N(1990)7/2^+$, is poor only.

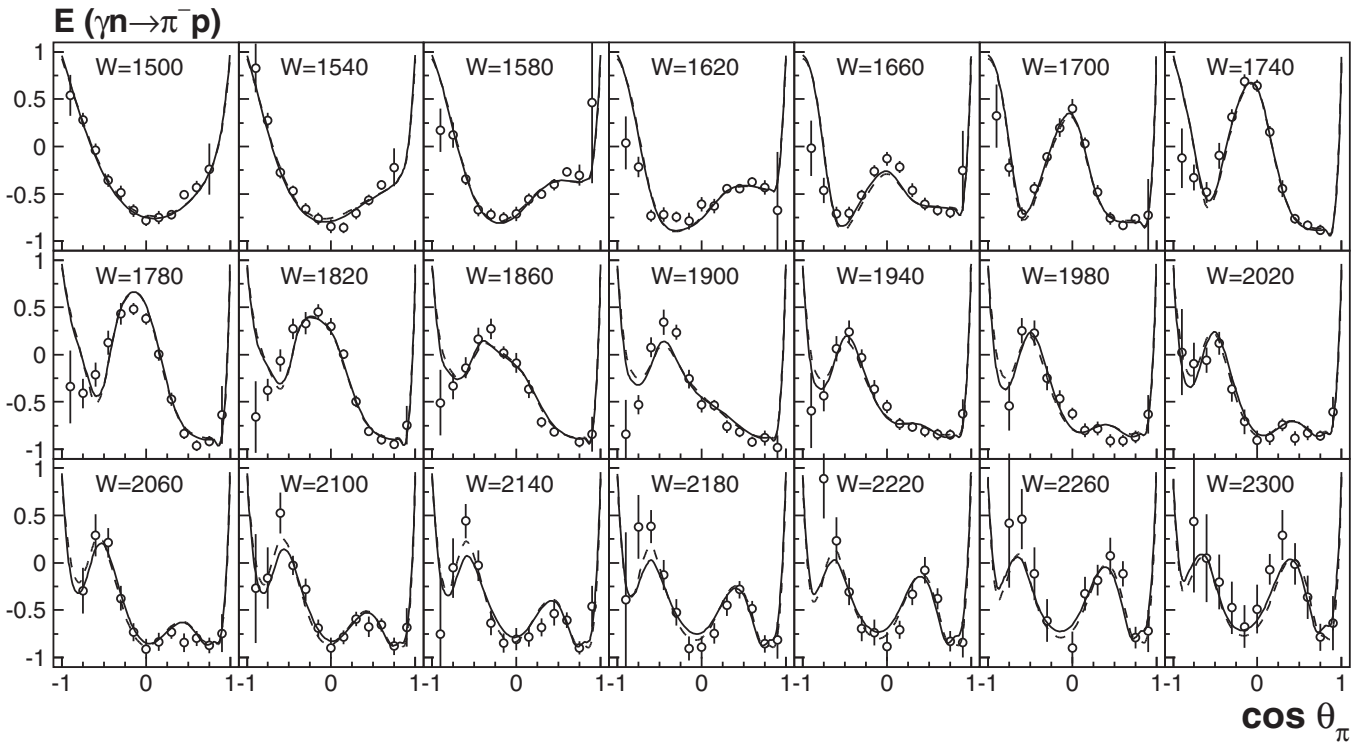

FIG. 2. E asymmetry for $\vec{\gamma}\vec{n} \to \pi^- p$ in bins of the invariant mass [21]. The solid and dashed curves show two BnGa fits.

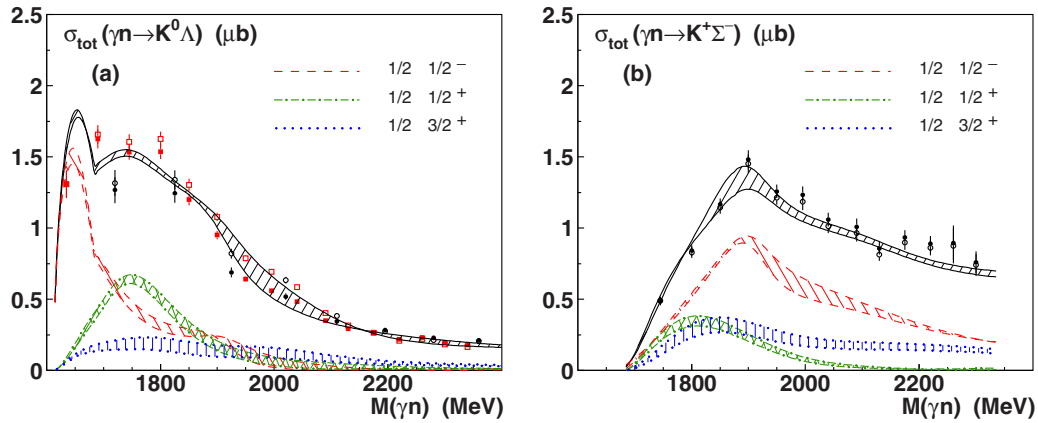

FIG. 3. Total cross sections for $\gamma d \to K^0\Lambda(p)$ [20] and $\gamma d \to K^+\Sigma^-(p)$ [22]. The contributions from three major partial waves with $I = 1/2$ and $J^P = 1/2^\pm$ and $3/2^+$ for the two major fits are also shown. Red squares and black circles represent data from the CLAS g10 and CLAS g13 experimental runs, respectively. Open and solid symbols represent the two fit results (see text).

To find realistic errors for the helicity amplitudes, we performed a series of eight fits (starting from both primary solutions) in which we added additional high-mass resonances with $J^P = 1/2^\pm$, $3/2^\pm$, $5/2^\pm$, and $7/2^\pm$ to the fit. The χ^2 did not improve significantly in any of these fits. The errors in the helicity amplitudes were determined from the spread in the results from the 18 fits (two principle solutions times nine variations).

Table II presents the resulting helicity and multipole couplings. The photon has helicity 1 and the nucleon helicity $1/2$ so that the total helicity can be $3/2$ or $1/2$. The electric E and magnetic multipole amplitudes are related to the two helicity amplitudes by [13]

$$E = \frac{1}{L+1}\left(A^{3/2}\sqrt{\frac{L}{L+2}} - A^{1/2}\right),$$
$$M = -\frac{1}{L+1}\left(A^{3/2}\sqrt{\frac{L+2}{L}} + A^{1/2}\right), \qquad (1)$$

for states with $J = L + \frac{1}{2}$ ($J^P = 1/2^-, 3/2^+, 5/2^-, \ldots$), and

$$E = -\frac{1}{L}\left(A^{3/2}\sqrt{\frac{L+1}{L-1}} + A^{1/2}\right),$$
$$M = -\frac{1}{L}\left(A^{3/2}\sqrt{\frac{L-1}{L+1}} - A^{1/2}\right), \qquad (2)$$

for states with $J = L - \frac{1}{2}$ ($J^P = 1/2^+, 3/2^-, 5/2^+, \ldots$). Here, L is the relative orbital angular momentum in the pseudoscalar meson-plus-baryon final state. In a Breit-Wigner parametrization, the helicity amplitudes have the conventional definition and are real numbers. When working in the complex plane, the helicity amplitudes at the pole position acquire phases.

The Breit-Wigner helicity amplitudes $A^{1/2}_{n(\mathrm{BW})}$ and $A^{3/2}_{n(\mathrm{BW})}$ and those at the pole position, $A^{1/2}_{n(\mathrm{pole})}$ and $A^{3/2}_{n(\mathrm{pole})}$, are calculated for the 18 fits described above using Eqs. (1) and (2). The results on the neutron helicity couplings of the $N(1700)3/2^-$ resonance are very unstable due to the presence of important thresholds like $K\Lambda$, $K\Sigma$, and ρN. Also the $N(1860)5/2^+$ properties are ill-defined. Hence we do not list the helicity couplings of these two resonances.

These helicity amplitudes are used to calculate the electric and magnetic amplitudes E and M, respectively. From the 18 values for $A^{1/2}$, $A^{3/2}$, E, and M, the mean values and their variance are determined. These results are listed in Table II.

First, we compare the new results on $A^n_{1/2}$ and $A^n_{3/2}$ with previously reported values (see Table III). There is approximate consistency (at the 2σ level) between all three analyses for all resonances below 1700 MeV. Only in the 1700- to 1800-MeV mass region Ref. [12] reports helicity amplitudes which are significantly different from our findings. We found $N(1700)3/2^-$ difficult to establish and do not give helicity amplitudes in this paper. Our previous result on $A^n_{1/2}$ for $N(1710)1/2^+$ [11] and the value from Ref. [12] have opposite signs. For $N(1710)1/2^+$, the $A^{1/2}$ value reported in Ref. [12] is about 5 times larger than our value; $A^{3/2}$ is reported to be -28 in Ref. [12] and 100 ± 35 in this work (consistent with 140 ± 65 reported in Ref. [11]. The $J^P = 3/2^+$ wave contains two resonances in Ref. [12]; we have no evidence for $N(1765)3/2^+$. Higher-mass resonances are not included in Ref. [12]; these often have small $N\pi$ couplings and are less important in reactions with $N\pi$ in the final state.

The origin of the discrepancies in the 1700- to 1800-MeV mass region could be the additional $N(1765)3/2^+$ resonance reported in Ref. [12]. It is found to have a strong $N\pi$ coupling, of the same size as $N(1520)3/2^-$. The latter resonance is strongly seen in πN elastic scattering. It needs to be shown that the P13 partial wave is compatible with an extra $N(1765)3/2^+$ resonance with strong $N\pi$ coupling.

In the region above 1800 MeV, most values from our new evaluation are not consistent with the values reported in Ref. [11]. We associate these changes with the inherent inconsistencies between the cross-section data that have been used here compared with those of previous analyses and with the new precise data on the helicity asymmetry E [21]. Figure 4 compares the excitation curve for $\gamma n \to \eta n$ reported

TABLE II. The γN helicity couplings of nucleon states (10^{-3} GeV$^{-1/2}$) calculated as residues in the pole position and the corresponding Breit-Wigner couplings [13].

	$A_{1/2}$	Phase	$A_{1/2}^{(\mathrm{BW})}$	$A_{3/2}$	Phase	$A_{3/2}^{(\mathrm{BW})}$	E	Phase	$E^{(\mathrm{BW})}$	M	Phase	$M^{(\mathrm{BW})}$
$N(1535)1/2^-$	-88 ± 4	$5^\circ\pm4^\circ$	-81 ± 6				88 ± 4	$5^\circ\pm4^\circ$	81 ± 6			
$N(1650)1/2^-$	16 ± 4	$-28^\circ\pm10^\circ$	16 ± 5				-16 ± 4	$-28^\circ\pm10^\circ$	-16 ± 5			
$N(1895)1/2^-$	-15 ± 10	$60^\circ\pm25^\circ$	-14 ± 10				15 ± 10	$60^\circ\pm25^\circ$	14 ± 10			
$N(1440)1/2^+$	41 ± 5	$23^\circ\pm10^\circ$	53 ± 7							41 ± 5	$23^\circ\pm10^\circ$	53 ± 7
$N(1710)1/2^+$	29 ± 7	$80^\circ\pm20^\circ$	$\pm(30\pm7)$							29 ± 7	$80^\circ\pm20^\circ$	$\pm(30\pm7)$
$N(1880)1/2^+$	72 ± 24	$-30^\circ\pm30^\circ$	70 ± 22							72 ± 24	$-30^\circ\pm30^\circ$	70 ± 22
$N(2100)1/2^+$	29 ± 9	$35^\circ\pm20^\circ$	29 ± 10							29 ± 9	$35^\circ\pm20^\circ$	29 ± 10
$N(1520)3/2^-$	-45 ± 5	$-5^\circ\pm4^\circ$	-46 ± 5	-119 ± 5	$5^\circ\pm4^\circ$	-118 ± 5	126 ± 5	$5^\circ\pm5^\circ$	125 ± 5	13 ± 3	$26^\circ\pm3^\circ$	13 ± 3
$N(1875)3/2^-$	4 ± 3	$-85^\circ\pm35^\circ$	$\pm(4\pm3)$	-6 ± 4	$-85^\circ\pm45^\circ$	$\pm(6\pm4)$	3 ± 2	$-50^\circ\pm40^\circ$	3 ± 2	3 ± 2	$-80^\circ\pm40^\circ$	$\pm(3\pm2)$
$N(2120)3/2^-$	80 ± 30	$15^\circ\pm25^\circ$	81 ± 30	-33 ± 20	$-60^\circ\pm35^\circ$	-32 ± 20	-33 ± 15	$75^\circ\pm40^\circ$	-33 ± 15	43 ± 20	$5^\circ\pm20^\circ$	43 ± 20
$N(1720)3/2^+$	$-(25^{+40}_{-15})$	$-75^\circ\pm35^\circ$	$-(28^{+40}_{-15})$	100 ± 35	$-80^\circ\pm35^\circ$	$\pm(103\pm35)$	(20^{+30}_{-10})	$-75^\circ\pm30^\circ$	(20^{+30}_{-10})	-85 ± 30	$-80^\circ\pm30^\circ$	$\pm(85\pm30)$
$N(1900)3/2^+$	-98 ± 20	$-13^\circ\pm20^\circ$	-102 ± 20	74 ± 15	$5^\circ\pm15^\circ$	73 ± 15	70 ± 17	$-8^\circ\pm20^\circ$	71 ± 17	-22 ± 12	$40^\circ\pm40^\circ$	-21 ± 11
$N(1975)3/2^+$	-26 ± 13	$8^\circ\pm25^\circ$	-26 ± 13	-77 ± 15	$5^\circ\pm20^\circ$	-75 ± 15	-12 ± 10	$-10^\circ\pm35^\circ$	-12 ± 9	80 ± 15	$5^\circ\pm20^\circ$	79 ± 14
$N(1675)5/2^-$	-53 ± 4	$-3^\circ\pm5^\circ$	-53 ± 4	-73 ± 5	$-12^\circ\pm5^\circ$	-72 ± 5	3 ± 2	$60^\circ\pm30^\circ$	3 ± 2	52 ± 5	$-10^\circ\pm5^\circ$	51 ± 4
$N(2060)5/2^-$	52 ± 25	$-5\pm20^\circ$	52 ± 24	12 ± 7	$-40^\circ\pm35^\circ$	12 ± 7	-21 ± 7	$3^\circ\pm15^\circ$	-20 ± 7	-29 ± 6	$3\pm20^\circ$	-29 ± 6
$N(1680)5/2^+$	32 ± 3	$-7^\circ\pm5^\circ$	33 ± 3	-63 ± 4	$-10^\circ\pm5^\circ$	-63 ± 4	19 ± 2	$-13^\circ\pm7^\circ$	19 ± 2	25 ± 2	$-9^\circ\pm4^\circ$	26 ± 2
$N(2000)5/2^+$	19 ± 10	$-80^\circ\pm40^\circ$	$\pm(19\pm10)$	11 ± 5	$82^\circ\pm30^\circ$	$\pm(11\pm5)$	$-(3^{+4}_{-3})$	Not defined	$-(3^{+4}_{-3})$	8 ± 4	$-86^\circ\pm30^\circ$	$\pm(8\pm4)$
$N(1990)7/2^+$	-32 ± 15	$5^\circ\pm20^\circ$	-32 ± 15	-70 ± 25	$0^\circ\pm20^\circ$	-72 ± 25	-7 ± 4	$-8^\circ\pm20^\circ$	-7 ± 4	31 ± 15	$-5^\circ\pm20^\circ$	31 ± 15
$N(2190)7/2^-$	30 ± 7	$5^\circ\pm15^\circ$	30 ± 7	-23 ± 8	$13^\circ\pm20^\circ$	-23 ± 8	1^{+3}_{-1}	$100^\circ\pm130^\circ$	1^{+3}_{-1}	12 ± 4	$8^\circ\pm12^\circ$	12 ± 4

TABLE III. Comparison of the γN helicity couplings of nucleon states (in units of 10^{-3} GeV$^{-1/2}$) from this analysis with those determined in Refs. [11] and [12]. In Ref. [12], no uncertainties are quoted. An "x" marks resonances not used in the fits. In some cases, for large errors of the couplings, the phase cannot be defined.

	$A_{1/2}$			Phase			$A_{3/2}$			Phase		
	This work	[11]	[12]	This work	[11]	[12]	This work	[11]	[12]	This work	[11]	[12]
$N(1535)1/2^-$	-88 ± 4	-103 ± 11	-112	$5^\circ\pm4^\circ$	$8^\circ\pm5^\circ$	16°						
$N(1650)1/2^-$	16 ± 4	25 ± 20	-1	$-28^\circ\pm10^\circ$	$0^\circ\pm15^\circ$	-47°						
$N(1875)1/2^-$	-15 ± 10	17 ± 10	x	$60^\circ\pm25^\circ$	$5^\circ\pm30^\circ$	x						
$N(1440)1/2^+$	41 ± 5	35 ± 12	95	$23^\circ\pm10^\circ$	$25^\circ\pm25^\circ$	-15°						
$N(1710)1/2^+$	29 ± 7	-40 ± 20	195	$80^\circ\pm20^\circ$	$-30^\circ\pm25^\circ$	-8°						
$N(1880)1/2^+$	72 ± 24	-60 ± 50	x	$-30^\circ\pm30^\circ$	$-30^\circ\pm40^\circ$	x						
$N(2100)1/2^+$	29 ± 9	x	x	$35^\circ\pm20^\circ$	x	x						
$N(1520)3/2^-$	-45 ± 5	-49 ± 8	-43	$-5^\circ\pm4^\circ$	$-3^\circ\pm8^\circ$	-1°	-119 ± 5	-114 ± 12	-110	$5^\circ\pm4^\circ$	$1^\circ\pm3^\circ$	5°
$N(1700)3/2^-$	x	31 ± 10	-40	x	$-50^\circ\pm30^\circ$	-46°	x	-35 ± 18	-77	x	$-30^\circ\pm30^\circ$	-57°
$N(1875)3/2^-$	4 ± 3	9 ± 6	x	$-85^\circ\pm35^\circ$	Not defined	x	-6 ± 4	-19 ± 15	x	$-85^\circ\pm45^\circ$	Not defined	x
$N(2120)3/2^-$	80 ± 30	112 ± 40	x	$15^\circ\pm25^\circ$	$30\pm25^\circ$	x	-33 ± 20	40 ± 30	x	$-60^\circ\pm35^\circ$	$-55^\circ\pm60^\circ$	x
$N(1720)3/2^+$	$-(25^{+40}_{-15})$	-80 ± 50	-59	$-75^\circ\pm35^\circ$	$-20^\circ\pm30^\circ$	6°	100 ± 35	-140 ± 65	-28	$-80^\circ\pm35^\circ$	$5^\circ\pm30^\circ$	-19°
$N(1765)3/2^+$	x	x	-34	x	x	-5°	x	x	40	x	x	6°
$N(1900)3/2^+$	-98 ± 20	-5 ± 35	x	$-13^\circ\pm20^\circ$	$30^\circ\pm30^\circ$	x	74 ± 15	-60 ± 40	x	$5^\circ\pm15^\circ$	$45^\circ\pm40^\circ$	x
$N(1975)3/2^+$	-26 ± 13	x	x	$8^\circ\pm25^\circ$	x	x	-77 ± 15	x	x	$5^\circ\pm20^\circ$	x	x
$N(1675)5/2^-$	-53 ± 4	-61 ± 7	-76	$-3^\circ\pm5^\circ$	$-10^\circ\pm5^\circ$	3°	-73 ± 5	-89 ± 10	-38	$-12^\circ\pm5^\circ$	$-17^\circ\pm7^\circ$	-4°
$N(2060)5/2^-$	52 ± 25	27 ± 12	x	$-5^\circ\pm20^\circ$	$-45^\circ\pm25^\circ$	x	12 ± 7	-40 ± 18	x	$-40^\circ\pm35^\circ$	$55^\circ\pm30^\circ$	x
$N(1680)5/2^+$	32 ± 3	33 ± 6	34	$-7^\circ\pm5^\circ$	$-12^\circ\pm9^\circ$	-12°	-63 ± 4	-44 ± 9	-56	$-10^\circ\pm5^\circ$	$8^\circ\pm10$	-4°
$N(2000)5/2^+$	19 ± 10	-17 ± 12	x	$-80^\circ\pm40^\circ$	$-50^\circ\pm60^\circ$	x	11 ± 5	-35 ± 20	x	$82^\circ\pm30^\circ$	$-50^\circ\pm90^\circ$	x
$N(1990)7/2^+$	-32 ± 15	-45 ± 20	x	$5^\circ\pm20^\circ$	$-50^\circ\pm35^\circ$	x	-70 ± 25	-50 ± 25	x	$0^\circ\pm20^\circ$	$-45^\circ\pm40^\circ$	x
$N(2190)7/2^-$	30 ± 7	-15 ± 12	x	$5^\circ\pm15^\circ$	$50^\circ\pm40^\circ$	x	-23 ± 8	-33 ± 20	x	$13^\circ\pm20^\circ$	$25^\circ\pm20^\circ$	x

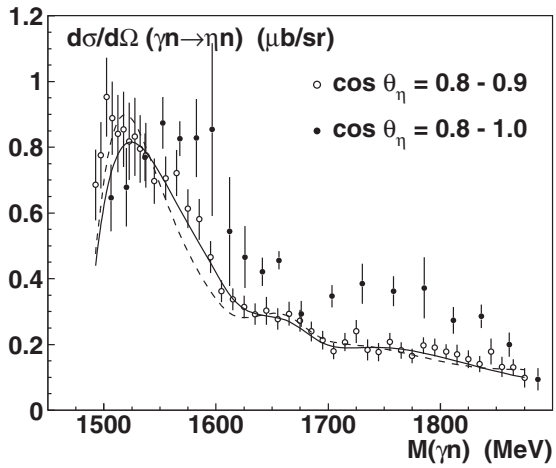

FIG. 4. The $\gamma d \to \eta n(p)$ excitation curve for the angular range $0.8 < \cos\theta < 0.9$ from the data from Refs. [15,16] (open circles, $0.8 < \cos\theta < 0.9$) and from Ref. [24] (black dots, $0.8 < \cos\theta < 1$). The solid and dashed curves show the two BnGa fits, which include the data from Refs. [15,16] but not the data from Ref. [24].

in Refs. [15,16] and the one reported in Ref. [24] at an angle of $\cos\theta = 0.85^\circ \pm 0.05^\circ$. Significant discrepancies are seen. We have decided to exclude the data from Ref. [24] completely and not to include fits to the latter data in the error analysis. (Our old result [11] is reproduced when the data from Refs. [20,22] are omitted and the new data [15,16] are replaced by the old data from Ref. [24].) We hence conclude that the changes in the helicity couplings for N^* resonances above 1800 MeV in mass are due to a decisive change in the data base, which has been improved considerably with new experiments.

IV. SEARCH FOR A NARROW RESONANCE

In the excitation function of η photoproduction from neutrons, a narrow structure was observed in a number of experiments [15–19,23–25]. The narrow structure was interpreted as $N(1685)$ [75] with preferred quantum numbers $J^P = 1/2^+$ and identified with a pentaquark expected in the chiral soliton model [5]. Its properties were determined [15,16] as $M = 1670 \pm 5$ and $\Gamma = 28 \pm 5$ MeV, respectively, and

$$\sqrt{b_\eta} A^n_{1/2} = 12.3 \pm 0.8 \times 10^{-3}\,\mathrm{GeV}^{-1/2}, \qquad (3)$$

with b_η being the branching ratio into the $N\eta$ final state.

The BnGa partial wave analysis has demonstrated that the narrow structure is incompatible with an interpretation as a genuine resonance with the reported properties [76,77]. Rather, full consistency is obtained by assuming that the peak is generated by the interference between the $N(1535)1/2^-$ and $N(1650)1/2^-$ resonances.

If an $N(1685)1/2^+$ resonance would exist and would be the expected pentaquark, it should be produced preferentially by exciting neutrons and should have large branching ratios to $N\eta$ and ΛK. We have searched for traces from an $N(1685)1/2^+$ resonance by introducing it as additional resonance. In this study, we have calculated the differential cross section

TABLE IV. The description of the data with fixed $\sqrt{b_{\Lambda K}} A^n_{1/2}$ for $N(1685)1/2^+$. The width of the state has been fixed to 28 MeV. The $*$ denotes that the parameter is at its boundary.

$\sqrt{b_{\Lambda K}} A^n_{1/2}$	M	χ^2	χ^2 $W < 1820$ MeV	χ^2
$(10^{-3}\,\mathrm{GeV}^{-1/2})$	MeV	$\gamma n \to K\Lambda$	$\gamma n \to K\Lambda$	Total
0.0	—	1.14	1.23	1.71
2.9	1665	1.07	1.25	1.70
4.4	1661	1.08	1.28	1.70
5.8	1654	1.11	1.30	1.71
7.8	1650*	1.19	1.34	1.72
11.	1650*	1.35	1.48	1.75
15.	1650*	1.80	1.96	1.85

assuming a narrow $N(1685)1/2^+$ resonance. Its mass has been incremented with a 1-MeV step size and the results from the corresponding rather broad energy bins have been compared with the experimental data. Below 30 MeV, the fits appear to be weakly sensitive only to the width of the state, and we have fixed it to 28 MeV. The fit with a free coupling, free mass, and free phase appear optimal for a mass of 1665 MeV and for $\sqrt{b_{\Lambda K}} A^n_{1/2} = 2.9 \times 10^{-3}\,\mathrm{GeV}^{-1/2}$, a rather small value. In this fit the description of the $\gamma n \to K\Lambda$ data in the mass region below 1820 MeV is slightly worse while the description of the high-energy region is improved as well as the overall χ^2 (see Table IV). If the coupling of the state is increased, the description of the data deteriorates, and the mass of the state hits the lower boundary. This low mass is incompatible with the observation in the ηn channel. For the strength of the signal we derive an upper limit of

$$\sqrt{b_{\Lambda K}} A^n_{1/2} < 6 \times 10^{-3}\,\mathrm{GeV}^{-1/2}, \qquad \Gamma = 28\ \mathrm{MeV}. \quad (4)$$

Compared to the claim for the ηn channel [15,16], we find

$$\frac{b_{\Lambda K}}{b_{n\eta}} < \frac{1}{4}. \qquad (5)$$

V. INTERPRETATION

Capstick and Roberts [78] have published a comprehensive review of the calculations of baryon properties, including helicity couplings. The predictions scatter over a wide range, and none of the models seems to be significantly better adapted to reproducing the experimental results. Here we try to interpret a few features.

It has been observed that $\Delta(1950)7/2^+$ is excited dominantly by the magnetic multipole M_{3+} with E_{3+}/M_{3+} being small [79]. This has been compared to photoexcitation of $\Delta(1232)3/2^+$, which is known to have a small E_{1+}/M_{1+} ratio. Both reactions require a spin flip from the spin-1/2 nucleon to a resonance with a total quark-spin $S = 3/2$ in the final state. It is this observation that has triggered us to decompose the well-known helicity amplitudes $A_{1/2}$ and $A_{3/2}$ into their electric and magnetic components (see Table II).

In most cases, the electric multipole amplitude is larger than the magnetic one; $E > M$ holds for most resonances. But there are a few cases where the magnetic multipole amplitude

TABLE V. Resonances with a small E/M ratio that are tentatively assigned to multiplets with quark-spin $S = 3/2$. The E/M ratios for γp reactions are given for comparison.

	$N(1675)5/2^-$	$N(1975)3/2^+$	$N(1990)7/2^+$	$N(2190)7/2^-$
$(E/M)_n$	0.06 ± 0.04	0.16 ± 0.08	0.19 ± 0.19	<0.35
$(E/M)_p$	< 0.27	—	< 0.2	0.57 ± 0.26

prevails, as in Table V. In Table V we also have included results for the E/M ratio for γp. (The proton helicity amplitudes are taken from the RPP2016 [80]).

It is tempting to interpret these states as members of spin quartets, with total quark-spins $S = 3/2$. This interpretation is justified for $N(1675)5/2^-$ and $N(1990)7/2^+$ and would assign $N(1975)3/2^+$—instead of $N(1900)3/2^+$—to a quartet of positive parity N^* resonances, with $N(1990)7/2^+$ as the anchor. The $N(2000)5/2^+$ resonance with $(E/M)_n = 0.4^{+1.4}_{-0.4}$ and $(E/M)_p = 0.50 \pm 0.24$ is the third candidate. The $N(1900)3/2^+$ resonance would then belong to a spin doublet. It is preferentially excited by its electric multipole, with $|(E/M)_n| = 3.4^{+3.8}_{-1.3}$. However, for the proton we find a smaller electric multipole, $(E/M)_p < 0.4$, and the assignment is thus questionable.

In most excitations, the resonances are excited by electric and magnetic multipoles. For N^* resonances photoexcited from protons, some N^* or Δ^* resonances that are likely assigned to a spin quartet can be excited dominantly by their electric multipole and weakly by the magnetic one. This would seem to contradict the conjecture that the excitation of resonances belonging to a spin quartet need a strong magnetic multipole. However, often the results from different analyses give substantially different results; the conjecture needs a better experimental and theoretical foundation.

Of course, electric excitation of spin-quartet states is at least possible due to LS coupling. Furthermore, most resonances assigned to a spin quartet could have a (quark) spin-1/2 component due to configuration mixing. Table VI reproduces from Ref. [3] the spectrum of positive-parity resonances in the second excitation shell. The table shows that the SU(6)⊗O(3) eigenstates may undergo very significant mixing. In particular the *stretched* resonances with maximal J $(= L + S)$ are nearly pure SU(6)⊗O(3) eigenstates. (The spin doublet from $^2N[20,1^+]$ is omitted in Table VI. In Refs. [74,81] it is argued that they are not likely to be produced in γN or πN formation experiments).

Montagne and Stancu [82] have analyzed the nucleon excitation spectrum in a $1/N_c$ expansion scheme. They expect a spin quartet in the SU(6) multiplet $^4N[70,2^+]$. Their masses (first row) and experimentally observed candidates (second row) are as follows:

2080 ± 39	2042 ± 41	1955 ± 32	1878 ± 34
$N(1990)7/2^+$	$N(2000)5/2^+$	$N(xxx)3/2^+$	$N(1880)1/2^+$.

No $^4N[70,2^+]$ state with $J^P = 3/2^+$ was assigned in Ref. [82]; we tentatively identify this state with $N(1975)3/2^+$.

TABLE VI. Positive-parity nucleon resonances in the second excitation shell [3]. On the left, the dominant multiplet is shown, and the fractional contribution of the dominant multiplet is given as a percentage below the predicted mass. The nominal masses from Table II are given in parentheses. The assignments are based on the predicted and experimental masses as well as on the observed E/M ratios and are tentative only.

	$7/2^+$	$5/2^+$	$3/2^+$	$1/2^+$
$^4 8[70,2^+]$	1989 (1990)	1934 (2000)	1899 (1975)	1950 (1880)
	98.1%	59.0%	93.9%	88.6%
$^2 8[70,2^+]$		1959 (1860)	1969 (1900)	
		67.4%	56.0%	
$^2 8[56,2^+]$		1723 (1680)	1688 (1720)	
		65.9%	66.6%	
$^4 8[70,0^+]$			2033 (miss)	
			54.3%	
$^2 8[70,0^+]$				1729 (1710)
				81.4%
$^2 8[56,0^+]$				1518 (1440)
				90.8%

Likewise, the SU(6) multiplet $^2N[70,2^+]$ is expected with masses of

1959 ± 29	1902 ± 22
$N(1860)5/2^+$	$N(1900)3/2^+$

and the identification with known states by the authors of Ref. [82] is again listed in the second row.

We mention here that Montagne and Stancu [82] also calculate the masses of the spin doublet in the SU(6) 56plet with $L = 2$, $^2N[56,2^+]$, to be 1680 ± 9 MeV $(3/2^+)$ and 1686 ± 5 MeV $(5/2^+)$; these resonances are identified with $N(1720)3/2^+$ and $N(1680)5/2^+$, respectively. The mass of the $^2N[70,0^+]$ spin-$3/2^+$ resonance is calculated to be 2024 ± 20 MeV; the latter resonance is assigned to the state $N(2040)3/2^+$ found by the BES Collaboration [83]. While the $N(1710)1/2^+$ resonance, likely a $^2N[70,0^+]$ spin-$1/2^+$ resonance, is thought not to exist, we in fact do see very clear evidence for it, and it is upgraded to a four-star resonance by the Particle Data Group [80]. The mass of the Roper resonance $N(1440)1/2^+$ in the $^2N[56,0^+]$ multiplet is not given. It seems that the model has problems with radial excitations. For the orbital excitations in the second shell it provides a useful framework.

VI. SUMMARY

We have reported the results of a new BnGa partial wave analysis of photoproduction reactions in deuterons with a spectator proton. Helicity amplitudes $A_{1/2}$ and $A_{3/2}$ and multipole amplitudes E and M are presented for 19 N^* resonances including the tentative $N(1975)3/2^+$ resonance. In the low-mass region, below 1800 MeV, most values from the new analysis are in good agreement with previously reported values. In the higher-mass region, significant changes in the

photocoupling constants are seen. These discrepancies are traced to inconsistencies of the new data from the CLAS and MAMI Collaborations with earlier experiments.

We have searched for possible contributions from $N(1685)$ to the reaction $\gamma n \to K^0\Lambda$, which is seen as a bump in the $\gamma n \to \eta n$ total cross section and sometimes interpreted as a resonance. We do not see evidence here and quote an upper limit for the product of its production amplitude and the square root of its decay branching ratio.

Some N^* resonances have a small E/M ratio. We have tentatively assigned these resonances to SU(6)⊗O(3) multiplets having a large quark-spin-3/2 component. This is a novel approach and needs confirmation. We have discussed the assignments of positive-parity N^* resonances, but the results remain ambiguous.

ACKNOWLEDGMENTS

We acknowledge financial support from the Deutsche Forschungsgemeinschaft (Grant No. SFB/TR110), the Russian Science Foundation (Grant No. 16-12-10267), and the US National Science Foundation (Grant No. 1306137). This material is in part based upon work supported by the US Department of Energy, Office of Science, Office of Nuclear Physics, under Contract No. DE-AC05-06OR23177.

[1] S. Capstick and N. Isgur, Phys. Rev. D **34**, 2809 (1986).
[2] M. Ferraris, M. M. Giannini, M. Pizzo, E. Santopinto, and L. Tiator, Phys. Lett. B **364**, 231 (1995).
[3] U. Löring, B. C. Metsch, and H. R. Petry, Eur. Phys. J. A **10**, 395 (2001).
[4] R. G. Edwards, J. J. Dudek, D. G. Richards, and S. J. Wallace, Phys. Rev. D **84**, 074508 (2011).
[5] D. Diakonov, V. Petrov, and M. V. Polyakov, Z. Phys. A **359**, 305 (1997).
[6] G. Penner and U. Mosel, Phys. Rev. C **66**, 055212 (2002).
[7] D. Drechsel, S. S. Kamalov, and L. Tiator, Eur. Phys. J. A **34**, 69 (2007).
[8] W. Chen *et al.*, Phys. Rev. Lett. **103**, 012301 (2009).
[9] P. Vancraeyveld, L. De Cruz, J. Ryckebusch, and T. Vrancx, Nucl. Phys. A **897**, 42 (2013).
[10] M. Shrestha and D. M. Manley, Phys. Rev. C **86**, 055203 (2012).
[11] A. V. Anisovich, V. Burkert, E. Klempt, V. A. Nikonov, A. V. Sarantsev, and U. Thoma, Eur. Phys. J. A **49**, 67 (2013).
[12] H. Kamano, S. X. Nakamura, T. S. H. Lee, and T. Sato, Phys. Rev. C **94**, 015201 (2016).
[13] R. L. Workman, L. Tiator, and A. Sarantsev, Phys. Rev. C **87**, 068201 (2013).
[14] M. Dieterle *et al.* (A2 Collaboration), Phys. Rev. Lett. **112**, 142001 (2014).
[15] D. Werthmüller *et al.* (A2 Collaboration), Phys. Rev. C **90**, 015205 (2014).
[16] D. Werthmüller *et al.* (A2 Collaboration), Phys. Rev. Lett. **111**, 232001 (2013).
[17] L. Witthauer *et al.* (A2 Collaboration), Phys. Rev. Lett. **117**, 132502 (2016).
[18] L. Witthauer *et al.* (A2 Collaboration), Phys. Rev. C **95**, 055201 (2017).
[19] L. Witthauer *et al.* (CBELSA/TAPS Collaboration), Eur. Phys. J. A **53**, 58 (2017).
[20] N. Compton *et al.* (CLAS Collaboration), arXiv:1706.04748 [Phys. Rev. C (to be published)].
[21] D. Ho *et al.* (CLAS Collaboration), Phys. Rev. Lett. **118**, 242002 (2017).
[22] S. A. Pereira *et al.* (CLAS Collaboration), Phys. Lett. B **688**, 289 (2010).
[23] V. Kuznetsov *et al.* (GRAAL Collaboration), Phys. Lett. B **647**, 23 (2007).
[24] I. Jaegle *et al.* (CBELSA and TAPS Collaborations), Phys. Rev. Lett. **100**, 252002 (2008).
[25] I. Jaegle *et al.*, Eur. Phys. J. A **47**, 89 (2011).
[26] J. J. Wu, T. Sato, and T.-S. H. Lee, Phys. Rev. C **91**, 035203 (2015).
[27] A. Fix and H. Arenhövel, Phys. Rev. C **72**, 064005 (2005).
[28] P. Benz *et al.* (ABHHM Collaboration), Nucl. Phys. B **65**, 158 (1973).
[29] V. Rossi *et al.*, Nuovo Cimento A **13**, 59 (1973).
[30] P. E. Argan *et al.*, Nucl. Phys. A **296**, 373 (1978).
[31] M. Beneventano *et al.*, Nuovo Cimento A **19**, 529 (1974).
[32] T. Fujii *et al.*, Nucl. Phys. B **120**, 395 (1977).
[33] G. Von Holtey, G. Knop, H. Stein, J. Stuempfig, and H. Wahlen, Nucl. Phys. B **70**, 379 (1974).
[34] G. Neugebauer, W. Wales, and R. L. Walker, Phys. Rev. **119**, 1726 (1960).
[35] P. E. Scheffler and P. L. Walden, Nucl. Phys. B **75**, 125 (1974).
[36] W. Chen, H. Gao, W. J. Briscoe, D. Dutta, A. E. Kudryavtsev, M. Mirazita, M. W. Paris, P. Rossi, S. Stepanyan, I. I. Strakovsky, V. E. Tarasov, and R. L. Workman, Phys. Rev. C **86**, 015206 (2012).
[37] F. V. Adamian *et al.*, J. Phys. G **15**, 1797 (1989).
[38] J. Alspector *et al.*, Phys. Rev. Lett. **28**, 1403 (1972).
[39] G. Knies *et al.*, Phys. Rev. D **10**, 2778 (1974).
[40] K. Kondo *et al.*, Phys. Rev. D **9**, 529 (1974).
[41] G. Mandaglio *et al.* (GRAAL Collaboration), Phys. Rev. C **82**, 045209 (2010).
[42] L. O. Abrahamian *et al.*, Sov. J. Nucl. Phys. **32**, 69 (1980).
[43] V. B. Ganenko *et al.*, Sov. J. Nucl. Phys. **23**, 511 (1976).
[44] F. F. Liu, D. J. Drickey, and R. F. Mozley, Phys. Rev. **136**, B1183 (1964).
[45] S. Hoblit, M. Khandaker, and A. M. Sandorfi (private communication).
[46] V. L. Agranovich *et al.*, Probl. At. Sc. Technol., Ser.: Nucl. Phys. Invest. **8**, 5 (1989).
[47] K. H. Althoff *et al.*, Nucl. Phys. B **96**, 497 (1975).
[48] K. H. Althoff *et al.*, Nucl. Phys. B **116**, 253 (1976).
[49] K. Fujii *et al.*, Nucl. Phys. B **187**, 53 (1981).
[50] H. Takeda *et al.*, Nucl. Phys. B **168**, 17 (1980).
[51] J. R. Kenemuth and P. C. Stein, Phys. Rev. **129**, 2259 (1963).
[52] M. Beneventano *et al.*, Nuovo Cimento **26**, 840 (1970).
[53] A. Bagheri, K. A. Aniol, F. Entezami, M. D. Hasinoff, D. F. Measday, J.-M. Poutissou, M. Salomon, and B. C. Robertson, Phys. Rev. C **38**, 885 (1988).

[54] J. C. Comiso *et al.*, Phys. Rev. D **12**, 719 (1975).
[55] G. J. Kim, J. Arends, W. J. Briscoe, J. Engelage, B. M. K. Nefkens, M. E. Sadler, and H. J. Ziock, Phys. Rev. D **40**, 244 (1989).
[56] A. Shafi *et al.* (Crystal Ball Collaboration), Phys. Rev. C **70**, 035204 (2004).
[57] M. T. Tran *et al.*, Nucl. Phys. A **324**, 301 (1979).
[58] Wang, Ph.D. thesis, TRIUMF, 1992.
[59] A. J. Weiss *et al.*, Nucl. Phys. B **101**, 1 (1975).
[60] J. C. Staŝko, B. Bassalleck, E. C. Booth, M. B. Chertok, D. Healey, R. Jacot-Guillarmod, M. A. Kovash, D. J. Mack, D. F. Measday, J. P. Miller, M. A. Moinester, D. Ottewell, M. A. Pickar, and P. Weber, Phys. Rev. Lett. **72**, 973 (1994).
[61] G. J. Kim, J. Engelage, B. M. K. Nefkens, H. J. Ziock, J. Arends, W. J. Briscoe, and M. E. Sadler, Phys. Rev. D **43**, 687 (1991).
[62] J. C. Alder, C. Joseph, J. P. Perroud, M. T. Tran, G. H. Eaton, R. Frosch, H. Hirschmann, S. Mango, J. W. McCulloch, P. Shrager, G. Strassner, P. Truöl, P. Weymuth, and P. Wiederkehr, Phys. Rev. D **27**, 1040 (1983).
[63] A. Ando *et al.* (unpublished).
[64] C. Bacci *et al.*, Phys. Lett. B **39**, 559 (1972).
[65] Y. Hemmi *et al.*, Nucl. Phys. B **55**, 333 (1973).
[66] C. R. Clinesmith, Ph.D. thesis, California Institute of Technology, 1967.
[67] R. Di Salvo *et al.*, Eur. Phys. J. A **42**, 151 (2009).
[68] A. Fantini *et al.*, Phys. Rev. C **78**, 015203 (2008).
[69] A. V. Anisovich *et al.*, Phys. Lett. B, **772**, 247 (2017).
[70] R. L. Workman, R. A. Arndt, W. J. Briscoe, M. W. Paris, and I. I. Strakovsky, Phys. Rev. C **86**, 035202 (2012).
[71] I. Denisenko *et al.*, Phys. Lett. B **755**, 97 (2016).
[72] A. V. Anisovich, R. Beck, E. Klempt, V. A. Nikonov, A. V. Sarantsev, and U. Thoma, Eur. Phys. J. A **48**, 15 (2012).
[73] A. V. Anisovich, E. Klempt, V. A. Nikonov, A. V. Sarantsev, and U. Thoma, Phys. Lett. B **711**, 167 (2012).
[74] V. Sokhoyan *et al.* (CBELSA/TAPS Collaboration), Eur. Phys. J. A **51**, 95 (2015); V. Sokhoyan, *ibid.* **51**, 187 (2015).
[75] V. Kuznetsov, EPJ Web Conf. **73**, 04020 (2014).
[76] A. V. Anisovich, E. Klempt, B. Krusche, V. A. Nikonov, A. V. Sarantsev, U. Thoma, and D. Werthmüller, Eur. Phys. J. A **51**, 72 (2015).
[77] A. V. Anisovich, V. Burkert, E. Klempt, V. A. Nikonov, A. V. Sarantsev, and U. Thoma, Phys. Rev. C **95**, 035211 (2017).
[78] S. Capstick and W. Roberts, Prog. Part. Nucl. Phys. **45**, S241 (2000).
[79] A. V. Anisovich *et al.*, Phys. Lett. B **766**, 357 (2017).
[80] C. Patrignani *et al.* (Particle Data Group), Chin. Phys. C **40**, 100001 (2016).
[81] A. Thiel *et al.* (CBELSA/TAPS Collaboration), Phys. Rev. Lett. **114**, 091803 (2015).
[82] N. Matagne and F. Stancu, Phys. Rev. D **93**, 096004 (2016).
[83] M. Ablikim *et al.* (BES Collaboration), Phys. Rev. D **80**, 052004 (2009).